BRAIN COMMUNICATIONS

Grey matter network trajectories across the Alzheimer's disease continuum and relation to cognition

Ellen Dicks,[1] Lisa Vermunt,[1] Wiesje M. van der Flier,[1,2] Frederik Barkhof,[3] Philip Scheltens[1] and Betty M. Tijms[1]; for the Alzheimer's Disease Neuroimaging Initiative[1]

*Data used in preparation of this article were obtained from the Alzheimer's Disease Neuroimaging Initiative (ADNI) database (adni.loni.usc.edu). As such, the investigators within the ADNI contributed to the design and implementation of ADNI and/or provided data but did not participate in analysis or writing of this report. A complete listing of ADNI investigators can be found at: http://adni.loni.usc.edu/wp-content/uploads/how_to_apply/ADNI_Acknowledgement_List.pdf

Biomarkers are needed to monitor disease progression in Alzheimer's disease. Grey matter network measures have such potential, as they are related to amyloid aggregation in cognitively unimpaired individuals and to future cognitive decline in predementia Alzheimer's disease. Here, we investigated how grey matter network measures evolve over time within individuals across the entire Alzheimer's disease cognitive continuum and whether such changes relate to concurrent decline in cognition. We included 190 cognitively unimpaired, amyloid normal (controls) and 523 individuals with abnormal amyloid across the cognitive continuum (preclinical, prodromal, Alzheimer's disease dementia) from the Alzheimer's Disease Neuroimaging Initiative and calculated single-subject grey matter network measures (median of five networks per individual over 2 years). We fitted linear mixed models to investigate how network measures changed over time and whether such changes were associated with concurrent changes in memory, language, attention/executive functioning and on the Mini-Mental State Examination. We further assessed whether associations were modified by baseline disease stage. We found that both cognitive functioning and network measures declined over time, with steeper rates of decline in more advanced disease stages. In all cognitive stages, decline in network measures was associated with concurrent decline on the Mini-Mental State Examination, with stronger effects for individuals closer to Alzheimer's disease dementia. Decline in network measures was associated with concurrent cognitive decline in different cognitive domains depending on disease stage: In controls, decline in networks was associated with decline in memory and language functioning; preclinical Alzheimer's disease showed associations of decline in networks with memory and attention/executive functioning; prodromal Alzheimer's disease showed associations of decline in networks with cognitive decline in all domains; Alzheimer's disease dementia showed associations of decline in networks with attention/executive functioning. Decline in grey matter network measures over time accelerated for more advanced disease stages and was related to concurrent cognitive decline across the entire Alzheimer's disease cognitive continuum. These associations were disease stage dependent for the different cognitive domains, which reflected the respective cognitive stage. Our findings therefore suggest that grey matter measures are helpful to track disease progression in Alzheimer's disease.

1 Alzheimer Center Amsterdam, Department of Neurology, Amsterdam Neuroscience, Vrije Universiteit Amsterdam, Amsterdam UMC, 1081 HV Amsterdam, The Netherlands
2 Department of Epidemiology and Biostatistics, Amsterdam Neuroscience, Vrije Universiteit Amsterdam, Amsterdam UMC, 1081 HV Amsterdam, The Netherlands

Received October 22, 2019. Revised June 23, 2020. Accepted July 02, 2020. Advance Access publication October 20, 2020

3 Department of Radiology and Nuclear Medicine, Amsterdam Neuroscience, Vrije Universiteit Amsterdam, Amsterdam UMC, 1081 HV Amsterdam, The Netherlands; Institutes of Neurology & Healthcare Engineering, UCL London, London WC1E, UK

Correspondence to: Ellen Dicks, PhD
Alzheimer Center and Department of Neurology,
Amsterdam UMC, PO Box 7057, 1007 MB Amsterdam,
The Netherlands
E-mail: e.dicks@amsterdamumc.nl; ellendicks.ac@gmail.com

Keywords: Alzheimer's disease; single-subject grey matter networks; graph theory; longitudinal; cognition

Abbreviations: ADNI = Alzheimer's Disease Neuroimaging Initiative; CN = controls; GM = grey matter; MMSE = Mini-Mental State Examination; RAVLT = Rey Auditory Verbal Learning Test; SUVR = standardized uptake value ratio; TMT = trail making test

Graphical Abstract

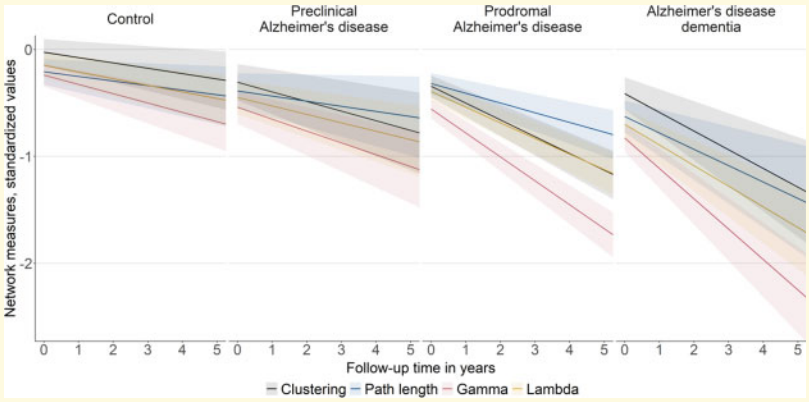

Introduction

Alzheimer's disease is a neurodegenerative disorder that is characterized by a progressive loss of cognitive functioning. The pathological cascade of Alzheimer's disease starts with the aggregation of amyloid beta up to 20 years before the onset of dementia (Bateman *et al.*, 2012; Jansen *et al.*, 2015). Once amyloid reaches abnormal levels, however, its absolute levels only show limited association with cognitive decline (Farrell *et al.*, 2017; Dubois *et al.*, 2018). Measures of neurodegeneration, such as hippocampal atrophy, are more strongly associated with cognitive decline and clinical progression (Fox *et al.*, 1999; Jack *et al.*, 2000; Dickerson *et al.*, 2009), but manifest relatively late in the disease process (Bateman *et al.*, 2012) and represent irreversible damage. Therapies targeted to treat Alzheimer's disease are probably most effective in the early stages of the disease, before overt and irreversible atrophy. For development of such secondary prevention trials, it is important to precisely and timely measure disease progression. To this end, biological substrates of cognitive dysfunction in early stages of the disease, when neurodegenerative changes are still subtle, are needed.

Normal cognitive function requires communication between different brain areas through their connections (i.e. brain connectivity). In Alzheimer's disease, amyloid impairs synaptic functioning (Walsh *et al.*, 2002; Shankar *et al.*, 2008; Koffie *et al.*, 2009), which may disrupt large-scale brain connectivity networks (Selkoe, 2002; Buckner *et al.*, 2005; Sperling *et al.*, 2009; Palmqvist *et al.*, 2017) and so early changes in brain connectivity patterns may represent an early link between amyloid aggregation and later cognitive decline in Alzheimer's disease. Brain connectivity can be measured based on similarity in grey matter (GM) (Mechelli *et al.*, 2005; Tijms *et al.*, 2012), which has been associated with coordinated growth during development (Alexander-Bloch *et al.*, 2013b), functional co-activation (Alexander-Bloch *et al.*, 2013a) and axonal connectivity (Gong *et al.*, 2012). We and others have previously shown that GM connectivity is disrupted in Alzheimer's disease (He *et al.*, 2008; Yao *et al.*, 2010, Tijms *et al.*, 2013a, *b*; Pereira *et al.*, 2016). In predementia stages, the level of GM network disruptions seems to lie in between those for cognitively normal and Alzheimer's disease dementia individuals (Yao *et al.*, 2010; Pereira *et al.*, 2016). Worse network disruptions are related to more severe cognitive impairment in Alzheimer's disease dementia (Tijms *et al.*, 2013a, 2014) and to the rate of future cognitive decline and clinical progression in predementia Alzheimer's disease (Dicks *et al.*, 2018; Tijms *et al.*, 2018; Verfaillie

et al., 2018). Disruptions in GM network measures have been shown to manifest already in cognitively normal individuals with the aggregation of amyloid (Tijms *et al.*, 2016; ten Kate *et al.*, 2018) but before overt atrophy (Voevodskaya *et al.*, 2018), suggesting these measures detect subtle structural changes in GM in the earliest stages of the disease due to amyloid aggregation. It could be hypothesized that the ongoing neurodegenerative changes throughout the disease might render the networks increasingly vulnerable, and thus represent a close biological substrate for cognitive decline and disease progression in Alzheimer's disease. Because amyloid preferentially starts to aggregate in distinct regions of the cortex (Villain *et al.*, 2012; Villeneuve *et al.*, 2015; Palmqvist *et al.*, 2017) and atrophy affects different regions of the brain (Whitwell *et al.*, 2007; Dickerson *et al.*, 2009), changes in network measures might show a distinct temporo-spatial pattern throughout the disease. While previous studies suggested that GM networks change as the disease progresses, those results were based on cross-sectional comparisons, and as such it remains unclear, how GM network measures evolve during the course of the disease.

Therefore, the objectives of this study were to investigate how GM network measures decline over time within individuals across the Alzheimer's disease cognitive continuum (i.e. cognitively unimpaired to dementia), how GM network measures are influenced by additional tau pathology and whether these changes translate to decline in specific cognitive domains *within* individuals.

Materials and methods

Participants

Data used in the preparation of this article were obtained from the Alzheimer's Disease Neuroimaging Initiative (ADNI) database (http://adni.loni.usc.edu). The ADNI was launched in 2003 as a public–private partnership, led by Principal Investigator Michael W. Weiner, MD. The primary goal of ADNI has been to test whether serial MRI, PET, other biological markers, and clinical and neuropsychological assessment can be combined to measure the progression of mild cognitive impairment and early Alzheimer's disease. ADNI was approved by the institutional review board of all participating institutions and written informed consent was obtained from all participants at each site.

We included all cognitively unimpaired, amyloid-normal individuals (controls; CN) and individuals with Alzheimer's disease across the cognitive continuum (preclinical, prodromal, Alzheimer's disease dementia) from ADNI, who had baseline amyloid biomarkers (PiB, AV45 PET or amyloid β 1–42 CSF) and ≥0.9 years of MRI follow-up available. A total of 713 individuals met inclusion criteria (190 CN, 100 preclinical, 288 prodromal, 135 Alzheimer's disease dementia). Criteria for clinical diagnoses in ADNI have been previously described (Petersen *et al.*, 2010). Briefly, clinical diagnoses were based on subjective memory complaints, the CDR, the Mini-Mental State Examination (MMSE) and education-adjusted cut-off values for the delayed recall of the Logical Memory II subscale of the Wechsler Memory Scale-Revised. Dementia patients additionally had to fulfil clinical diagnostic criteria for probable dementia according to the National Institute of Neurological and Communicative Disorders and Stroke–Alzheimer's Disease and Related Disorders Association criteria for probable Alzheimer's disease (McKhann *et al.*, 1984). Individuals with abnormal amyloid diagnosed as 'early' or 'late' mild cognitive impairment in ADNI were combined into the prodromal AD group.

Amyloid status at baseline was determined based on PiB or AV45 PET (http://adni.loni.usc.edu/methods/pet-analysis/; Jagust *et al.*, 2010, 2015), if available, and otherwise based on amyloid β 1–42 CSF levels (Shaw *et al.*, 2009). To determine amyloid abnormality, we used the recommended cut-offs of >1.5 standardized uptake value ratio (SUVR) for PiB ($n = 4$, 0.6% available), >1.1 SUVR for AV45 ($n = 476$, 66.8% available) (for both SUVRs the cerebellum was used as reference region; Jagust *et al.*, 2010, 2015) and <192 pg/ml for amyloid β 1–42 CSF levels ($n = 663$, 93% available) (Shaw *et al.*, 2009).

MRI acquisition and preprocessing

We downloaded all available 3D T_1-weighted scans with minimal preprocessing by ADNI from the ADNI LONI Image & Data Archive (IDA) [date of last access: 29 March 2017]. Within individuals, scans were only included when they had the same field strength. Details of image acquisition and initial preprocessing by ADNI have been previously described by Jack *et al.* (2008) (see also http://adni.loni.usc.edu/methods/mri-analysis/) and further image processing for this study are described in detail by Dicks *et al.* (2019). Briefly, longitudinal scans within individuals were co-registered to a subject-specific median template image (Reuter *et al.*, 2012) and then segmented into GM, white matter and cerebrospinal fluid using SPM12. Using the subject-specific inversed normalization parameters, we warped the automated anatomical labelling atlas (Tzourio-Mazoyer *et al.*, 2002) from standard space to subject space. GM volumes were calculated for each of the 90 regional cortical and subcortical automated anatomical labelling areas. Total intracranial volume was computed as the sum of grey and white matter and cerebrospinal fluid in cubic centimetre. A total of 3523 scans were of sufficient quality with a median number of 5 (IQR; 4–6) MRI scans per individual over a median follow-up of 2 (2–4) years. From all individual GM segmentation, we extracted single-subject GM networks using an automated method that has been previously

described (https://github.com/bettytijms/Single_Subject_Grey_Matter_Networks; Tijms *et al.*, 2012).

Grey matter network measures

For each network reconstructed from each scan, we calculated the network size, degree, connectivity density, clustering coefficient, path length and small-world measures (i.e. gamma, lambda) [for an overview of the measures see Rubinov and Sporns (2010)]. The network size corresponds to the number of nodes in the network and the degree indicates the average number of connections per node. Connectivity density is the ratio of the number of existing connections to the number of connections possible in the network. The clustering coefficient is the proportion of connected nodes that are also interconnected. Path length measures the average number of connections along the shortest path between every pair of nodes in the network. We further computed small-world measures in order to investigate how the network topology deviated from randomly generated networks: We used the corresponding values of five randomized networks with preserved degree distribution (Maslov and Sneppen, 2002) to calculate normalized values of the clustering coefficient (gamma) and path length (lambda). Local values of the degree, clustering and path length were computed by averaging the values over the corresponding nodes of each automated anatomical labelling area and global values were computed by averaging the values for all nodes over the entire network. For all network measures, we used the functions of the Brain Connectivity Toolbox adjusted for large-sized networks (https://sites.google.com/site/bctnet/; Rubinov and Sporns, 2010).

Neuropsychological assessments

We used the immediate and delayed recall subtests of the Rey Auditory Verbal Learning Test (RAVLT) (Rey, 1964), category fluency (animals), the trail making test (TMT) (Reitan, 1958) part A, TMT B and the MMSE (Folstein *et al.*, 1975) available in ADNI as measures for memory, language, attention/executive functioning and disease severity, respectively. For analyses investigating whether changes in network measures were associated with concurrent cognitive decline over time within individuals, we included only those individuals from our total sample who had $\geq$0.9 years of follow-up of both the respective neuropsychological assessment and MRI scans available. A total of 3049 assessments were available for the RAVLT, 3081 assessments for category fluency, 2935 assessments for the TMT and 3092 assessments for the MMSE. For all neuropsychological tests, the median number of assessments per individual was 4 (IQR; 3–5) over a median follow-up time of 2 (2–4) years.

Statistical analysis

Differences in baseline characteristics between diagnostic groups were assessed with one-way ANOVA, Kruskal–Wallis or chi-squared tests, where appropriate. If significant differences were found, we performed *post hoc* comparisons with Tukey's or Dunn's tests adjusted for multiple comparisons with the Hochberg procedure.

We fitted two sets of Bayesian linear mixed models with subject-specific intercepts and slopes with the package 'rstanarm' (Goodrich et al., 2020): we first assessed how network measures changed over time (model 1) and then investigated whether changes in network measures were associated with concurrent change in cognition within individuals (model 2). For model 1, follow-up time in years was entered as predictor and longitudinal network measures (NM) were included as outcome.

$$\mathrm{NM} = \beta_{\mathrm{Intercept}} + \beta_{\mathrm{Time}}\mathrm{Time} + (1 + \mathrm{Time}|\mathrm{Subject})$$

We repeated model 1 for local network measures for each of the 90 automated anatomical labelling areas, correcting for longitudinal local GM volume.

For model 2, longitudinal network measure was entered as predictor and longitudinal cognitive test score was entered as outcome.

$$\mathrm{Cognition} = \beta_{\mathrm{Intercept}} + \beta_{\mathrm{NM}}\mathrm{NM} + (1 + \mathrm{NM}|\mathrm{Subject})$$

Both sets of models additionally included baseline diagnosis (i.e. CN, preclinical, prodromal, Alzheimer's disease dementia) as a main term and an interaction effect with the predictor in order to investigate whether changes in network measures over time or associations with cognition depended on the baseline disease stage and in this way also approximated non-linear changes during the disease course. All analyses were corrected for age at baseline, sex, field strength and baseline total GM volume. Baseline total GM volume was excluded for network size and degree due to the high correlation between these measures. For associations with concurrent decline in cognition (model 2), we additionally corrected for educational level. All network measures and neuropsychological test scores were standardized to the mean values of CN group at baseline. Estimated marginal means and trends, and group differences between baseline disease stages were estimated with the emmeans package (Lenth, 2018).

All models except for network size and degree were run using eight independent chains with 10 000 iterations after 5000 initial warm-up samples. The final posterior sample consisted of 4000 draws. In models for network size and degree, we increased iterations to 15 000 with 7500 warm-up samples because not all iterations initially converged as indicated by the Gelman and Rubin (1992) potential scale reduction factor (Gelman and Shirley, 2011). For all models, we used a Cauchy distribution as prior for the intercept and each fixed effect. Effects were considered statistically significant if the 95% credible

interval (95% CI) of the posterior distribution did not overlap zero.

In order to assess whether additional tau pathology influences GM network measures in Alzheimer's disease individuals, we fitted two sets of linear mixed models with subject-specific random intercepts and slopes with the package 'lme4'. For the first set of models, we used continuous baseline CSF total tau levels, follow-up time in years and their interaction (i.e. baseline CSF total tau levels × follow-up time in years) as predictor and longitudinal network measures as outcome. For the second set of models, we used dichotomized baseline CSF total tau (i.e. normal/abnormal), follow-up time in years and their interaction (i.e. baseline CSF total tau status × follow-up time in years) as predictor and longitudinal network measures as outcome. Both sets of models were repeated for each Alzheimer's disease diagnostic group and were adjusted for age, sex, field strength and total GM volume.

All statistical analyses were performed in R (version 3.4.4, 2018-03-15) and Surf Ice (version 2017-08-08) was used to visualize regional results.

Data availability

The data used for this study were obtained from the ADNI database (adni.loni.usc.edu).

Results

The total sample included 713 individuals: 190 CN, 100 preclinical, 288 prodromal and 135 Alzheimer's disease dementia individuals (Table 1). The preclinical Alzheimer's disease group included more females than the prodromal Alzheimer's disease group and individuals with preclinical Alzheimer's disease were older than CN or prodromal Alzheimer's disease individuals ($P < 0.05$). CN showed higher years of education than individuals with prodromal Alzheimer's disease or Alzheimer's disease dementia ($P < 0.05$). CSF amyloid beta 1–42 levels and GM volumes were lowest and CSF total tau levels highest for Alzheimer's disease dementia individuals followed by prodromal Alzheimer's disease, preclinical Alzheimer's disease and CN individuals ($P < 0.05$). Alzheimer's disease dementia individuals had the shortest follow-up time with the fewest MRI scans available and CN and preclinical Alzheimer's disease individuals additionally had fewer MRI scans than individuals with prodromal Alzheimer's disease available ($P < 0.05$).

Longitudinal changes in cognitive performance over time by baseline disease stage are shown in Fig. 1 (see also Supplementary Fig. 1 and Tables 1 and 2). As expected, CN individuals and individuals with preclinical Alzheimer's disease showed the least impairment in cognition at baseline and the slowest cognitive decline, followed by prodromal Alzheimer's disease and then Alzheimer's disease dementia in all neuropsychological tests. Across neuropsychological tests, decline was most pronounced for the MMSE and attention/executive functioning in individuals with Alzheimer's disease dementia.

Cross-sectional differences and within-individual changes in GM network measures

At baseline, individuals with Alzheimer's disease dementia showed lower network size compared to prodromal Alzheimer's disease (Figs 2 and 3A; see also Supplementary Table 3). Alzheimer's disease dementia individuals showed the lowest path length values compared to all other groups. For gamma and lambda, baseline values were highest for CN individuals, followed by preclinical and prodromal Alzheimer's disease, and then Alzheimer's disease dementia. Cross-sectional results of local network measures largely reflected those for global network measures (see Supplementary Figs 2 and 3).

Over time, all network measures, except connectivity density, significantly declined within individuals of all groups, with fastest decline in gamma and lambda, followed by clustering, then path length and finally basic network measures (i.e. size, degree, connectivity density; see Figs. 2 and 3B; Supplementary Table 4 and also Supplementary Fig. 4 for individual-specific line plots). The rate of decline in network measures depended on individuals' cognitive stage, with decline in network measures generally accelerating with advancing disease stages: Network size and degree declined similarly in CN and preclinical Alzheimer's disease individuals, and then accelerated significantly in prodromal Alzheimer's disease and Alzheimer's disease dementia individuals, indicating acceleration in later disease stages in these measures. Connectivity density declined only in individuals with preclinical and prodromal Alzheimer's disease, but showed similar rates of decline. Decline in clustering and gamma was slowest in CN individuals, slightly accelerated for preclinical Alzheimer's disease and significantly accelerated in prodromal and dementia stages, suggesting an accelerating decline early in the disease process. Additionally, decline in gamma was significantly faster in Alzheimer's disease dementia than prodromal Alzheimer's disease, suggesting increasingly faster rates of decline in gamma values throughout the course of the disease. Decline in path length and lambda values was similar for CN and preclinical Alzheimer's disease individuals and then declined significantly faster for prodromal Alzheimer's disease and Alzheimer's disease dementia individuals, indicating an acceleration of decline in later disease stages.

When we repeated analyses correcting for longitudinal whole-brain GM volume, effects were attenuated, with only those in prodromal Alzheimer's disease remaining

Table 1 Demographic and clinical characteristics of the included sample and by baseline disease stage

	Total ($n = 713$)	CN ($n = 190$)	Preclinical Alzheimer's disease ($n = 100$)	Prodromal Alzheimer's disease ($n = 288$)	Alzheimer's disease dementia ($n = 135$)
Female	342 (48%)	90 (47%)	64 (64%)	124 (43%)[b]	64 (47%)
Age in years	73.5 (6.65)	72.55 (5.95)[b]	75.44 (5.57)	73.19 (6.91)[b]	74.08 (7.43)
Education in years	16 (14–18)	16 (15–18)	16 (14–18)	16 (14–18)[a]	16 (13–18)[a]
Progression to MCI	40 (6%)	21 (11%)	19 (19%)	n.a.	n.a.
Progression to dementia	159 (22%)	5 (3%)	7 (7%)	147 (51%)	n.a.
APOE4 allele (0/≥1)	328 (46%) /385 (54%)	151 (79%) /39 (21%)[b, c, d]	53 (53%) /47 (47%)[c, d]	96 (33%) /192 (67%)[d]	28 (21%) /107 (79%)
PiB PET SUVR[e]	1.88 (0.27)	n.a.	n.a.	1.88 (0.33)	1.89 (n.a.)
Abnormal PiB PET >1.5 SUVR[e]	4 (100%)	n.a.	n.a.	3 (100%)	1 (100%)
AV45 PET SUVR[f]	1.28 (0.22)	1.02 (0.05)[b, c, d]	1.34 (0.18)[d]	1.38 (0.16)[d]	1.45 (0.16)
Abnormal AV45 PET >1.11 SUVR[f]	333 (70%)	0 (0%)	70 (100%)	189 (100%)	74 (100%)
CSF Aβ 1–42 in pg/ml[g]	163.01 (50.41)	229.86 (38.22)	153.33 (35.36)[a]	139.95 (27.17)[a, b]	129.23 (21.33)[a, b, c]
Abnormal Aβ 1–42 < 192 pg/ml[g]	497 (75%)	29 (17%)[b, c, d]	81 (87%)[c, d]	263 (96%)[d]	124 (100%)
CSF total tau in pg/ml[g]	96.93 (54.03)	58.99 (23.83)[b, c, d]	77.71 (36.49)[c, d]	110.47 (52.7)[d]	133.63 (60.79)
Abnormal tau >93 pg/ml[g]	291 (44%)	19 (11%)[b, c, d]	27 (29%)[c, d]	153 (56%)[d]	92 (74%)
Follow-up time in years	2 (2–4)	2.2 (2–4)	2.1 (2–4)	3 (2–4)	1.5 (1–2)[a, b, c]
Number of MRI scans	5 (4–6)	5 (4–6)[c]	5 (3.2–6)[c]	5 (4–6)	4 (4–4)[a, b, c]
Field strength (3T)	2303 (69%)	666 (77%)	315 (73%)	997 (67%)	325 (59%)[a]
Total intracranial volume in cm^3	1452.91 (146.18)	1455.99 (140.97)	1435.76 (140.14)	1463.19 (145.29)	1439.36 (158.58)
Grey matter volume in cm^3	592.38 (71.79)	618.61 (59.66)	597.74 (66.4)	593.53 (71.32)[a]	549.01 (72.93)[a, b, c]
Normalized GM volume in cm^3	408.86 (41.38)	426.29 (34.69)	417.47 (36.81)	406.75 (40.97)[a]	382.45 (40.06)[a, b, c]
Hippocampal volume in cm^3	7.86 (1.44)	8.78 (1.03)	8.36 (0.96)[a]	7.71 (1.3)[a, b]	6.54 (1.42)[a, b, c]

Data are presented as *N* (%), mean (SD) or median (Q1–Q3), where appropriate.
[a]Higher for CN.
[b]Higher for preclinical Alzheimer's disease.
[c]Higher for prodromal Alzheimer's disease.
[d]Higher for Alzheimer's disease dementia.
[e]Available for $n = 4$.
[f]Available for $n = 476$.
[g]Available for $n = 663$.
n.a., not applicable.

significant (Supplementary Figs 5 and 6 and Tables 5 and 6).

On a regional level, correcting for concurrent local atrophy (Fig. 4; see also Supplementary Fig. 7 for group differences), the local degree most consistently declined, with the decline manifesting in the temporal lobes in CN individuals, additionally including most prominently the cingulate cortices in preclinical Alzheimer's disease individuals and then further affecting more frontal areas in individuals with prodromal Alzheimer's disease. At the same time, the local degree in mostly parietal regions increased in all three groups. For Alzheimer's disease dementia individuals, we further found almost exclusively increases over time in the local degree, particularly in the bilateral hippocampi. For the local clustering coefficient, we found mostly decline over time, with relatively little decline manifesting in CN individuals mostly restricted to parietal regions, and increasingly widespread effects in preclinical and prodromal Alzheimer's disease individuals. For Alzheimer's disease dementia individuals, decline in local clustering values was steeper compared to the other groups, and restricted to mostly fronto-parietal regions. For the local path length, similar to the other network measures, decline manifested in few regions in CN individuals, including the left precuneus and superior frontal gyrus, and became increasingly widespread in preclinical and then prodromal Alzheimer's disease. Additionally, we found an increase in path length values over time, most consistently in the right parahippocampal gyrus in CN and prodromal Alzheimer's disease individuals, but not in individuals with preclinical Alzheimer's disease or Alzheimer's disease dementia. For Alzheimer's disease dementia, similarly to the local clustering coefficient, the decline in path length values that were observed was

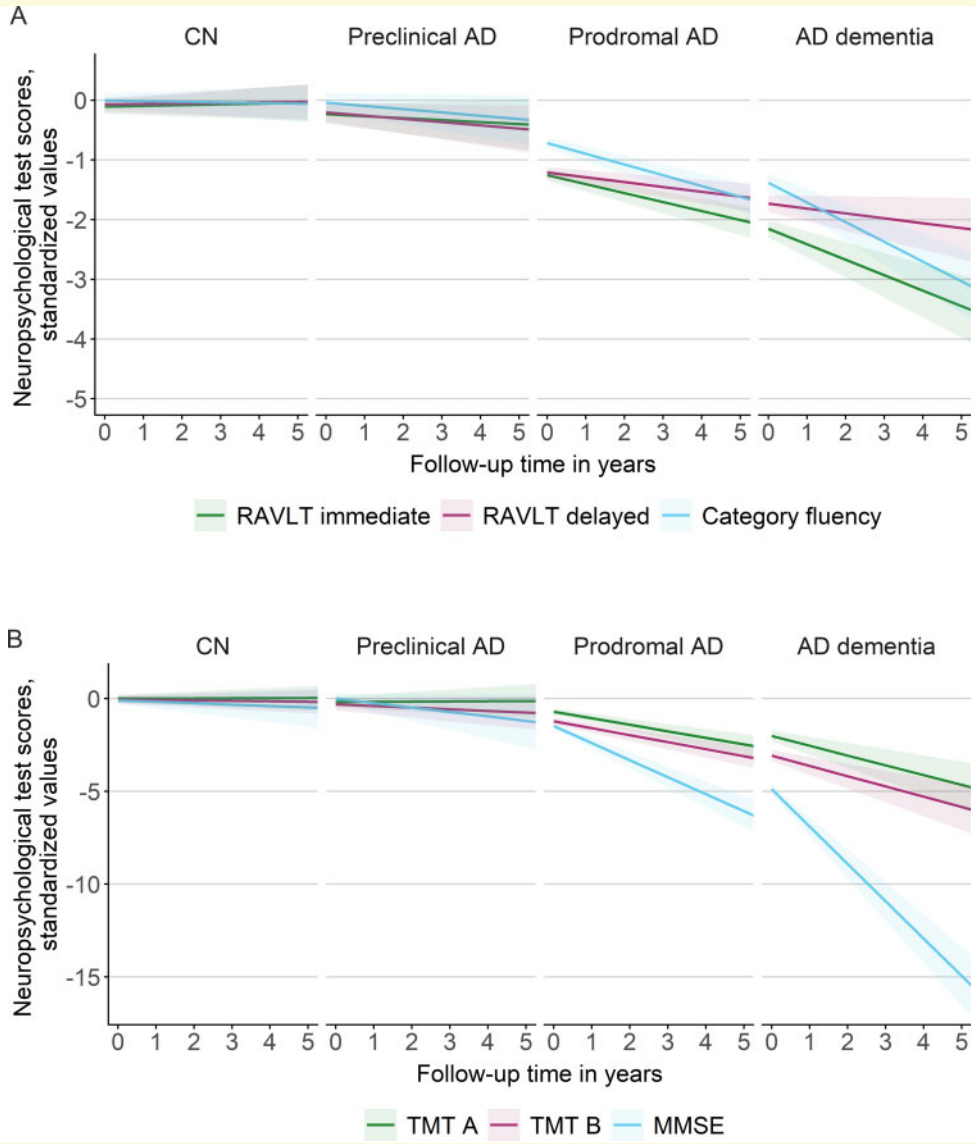

Figure 1 Longitudinal changes in neuropsychological test scores over time by baseline disease stage. Changes in MMSE, RAVLT immediate and delayed recall (**A**) and changes in TMT A, B and category fluency performance (**B**). Regression lines are based on estimated marginal means (intercept) and trends (slope) per baseline disease stage as modelled with Bayesian linear mixed models. The shaded area represents 95% credible intervals. Note that scores for TMT were inverted, so that lower scores indicate worse performance. Intercept and slope estimates can additionally be found in Supplementary Fig. 1 and Tables 1 and 2. AD, Alzheimer's disease.

steeper, but restricted to fewer regions, partly reflecting those regions that showed increasing values of the local degree in the same group of individuals.

We additionally investigated whether GM network disruptions in individuals with Alzheimer's disease were associated with tau pathology (Supplementary Tables 7–9). Cross-sectionally, higher baseline levels of total tau were associated with lower baseline network size and degree in prodromal Alzheimer's disease and lower baseline degree, connectivity density and clustering in Alzheimer's disease dementia. Longitudinally, higher baseline tau was associated with faster decline in lambda in preclinical Alzheimer's disease and faster decline in degree and clustering values in prodromal Alzheimer's disease. For Alzheimer's disease dementia, lower baseline tau was associated with faster decline in lambda values. When we repeated analyses for Alzheimer's disease dementia excluding one individual with noticeably low tau and fast decline in lambda (see Supplementary Fig. 8), the association between tau and lambda was greatly reduced and no longer significant ($\beta \pm SE = 0.001 \pm 0.0005$; $P = 0.07$).

Using tau status (normal/abnormal) as predictor instead of continuous values, we observed similar results for individuals with preclinical Alzheimer's disease (see Supplementary Tables 10–13): preclinical Alzheimer's

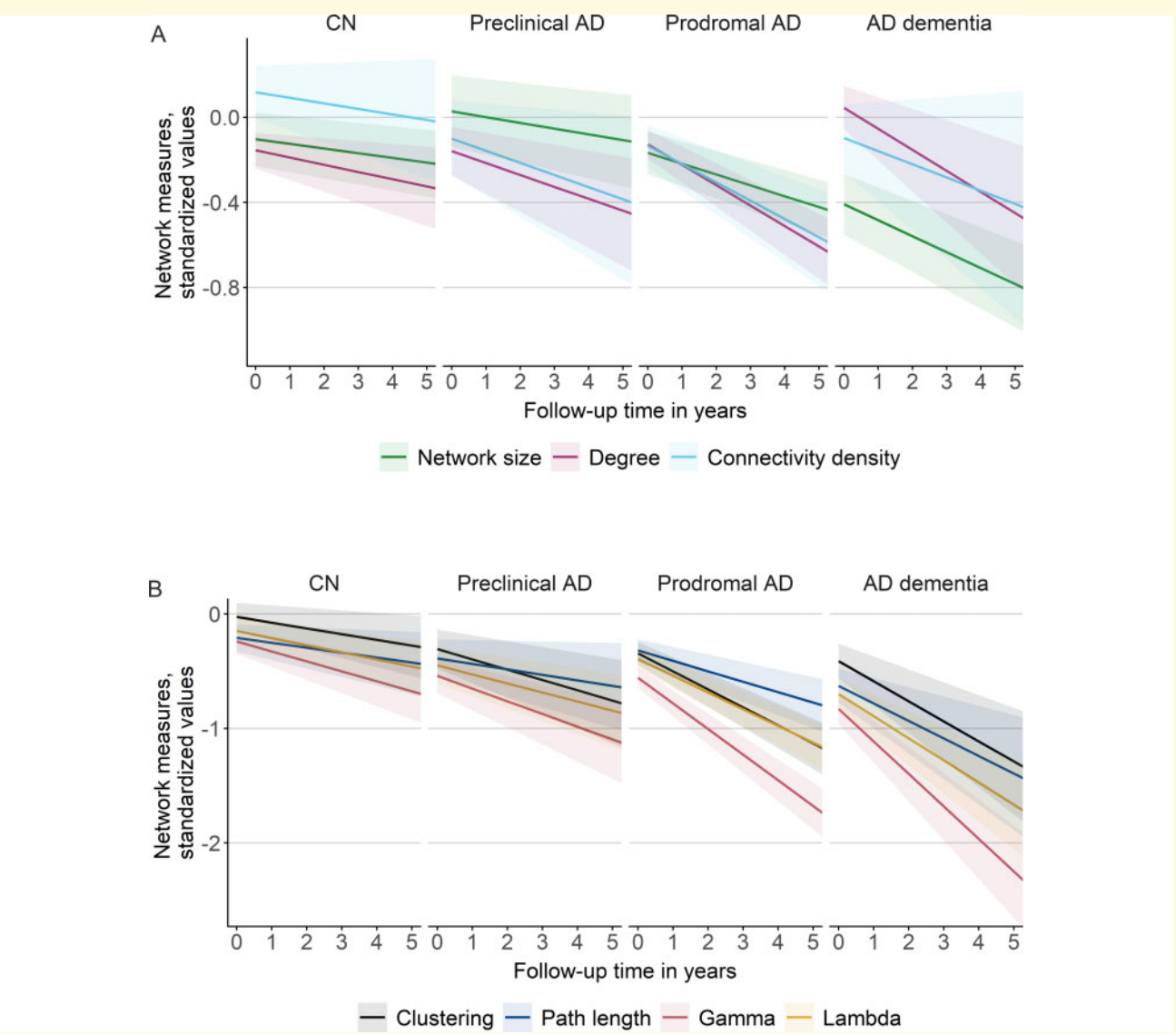

Figure 2 Longitudinal changes in global network measures over time by baseline disease stage. Changes in network size, degree and connectivity density (**A**) and changes in clustering, path length, gamma and lambda values (**B**). Regression lines are based on estimated marginal means (intercept) and trends (slope) per baseline disease stage as modelled with Bayesian linear mixed models. The shaded area represents 95% credible intervals. Intercept and slope estimates can additionally be found in Fig. 3 and Supplementary Tables 3 and 4. AD, Alzheimer's disease. Gamma is normalized clustering; lambda is normalized path length.

disease individuals with abnormal tau showed steeper rates of decline in path length and lambda compared to preclinical Alzheimer's disease individuals with normal tau levels. Together, these results suggest that additional tau pathology accelerates the decline in network measures particularly in the predementia stages of the disease.

Associations of within-individual change in network measures and concurrent cognitive decline

We further investigated whether decline in network measures was related to concurrent decline in cognition within individuals. We found several associations between changes in network measures and cognitive decline over time within individuals of all groups, with decline in network measures, most prominently gamma and lambda, being related to concurrent decline in distinct cognitive domains depending on disease stage (Fig. 5; see also Supplementary Table 14): In CN individuals, decline in network measures was associated with concurrent decline in memory (RAVLT immediate: network size, clustering; RAVLT delayed: connectivity density, clustering and gamma), language (category fluency: clustering and gamma) and MMSE (gamma). For preclinical Alzheimer's disease, the association between decline in network measures and concurrent memory decline was slightly stronger

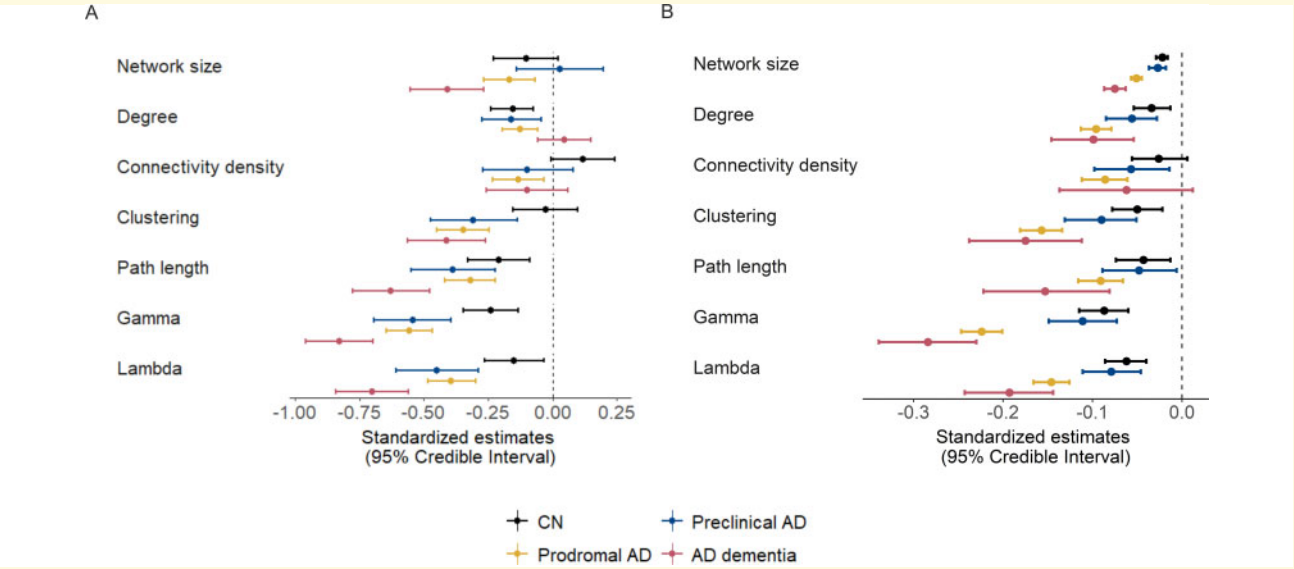

Figure 3 Cross-sectional and longitudinal effects in global network measures by baseline disease stage. Cross-sectional effects are shown in **A** and longitudinal effects are shown in **B** and are based on estimated marginal means and trends, respectively, as modelled with Bayesian linear mixed models. The error bars represent 95% credible intervals. Effects were considered significant if the 95% credible interval did not cross zero. Group differences were considered significant if the 95% credible interval of the pairwise group comparison did not cross zero and effects for the respective groups were significant. Estimates can additionally be found in Supplementary Tables 3 and 4. AD, Alzheimer's disease. Gamma is normalized clustering; lambda is normalized path length.

compared to CN (RAVLT immediate and delayed: path length, gamma and lambda), and we observed associations of decline in network measures and decline in attention/executive functioning (TMT B: gamma, lambda) and decline in network measures was additionally related to decline in language functioning (path length, lambda) and the MMSE (gamma, lambda). In prodromal Alzheimer's disease, these associations were generally stronger than for preclinical Alzheimer's disease, with decline in all network measures and most prominently gamma and lambda, showing associations with concurrent decline in all cognitive domains. In Alzheimer's disease dementia, we found fewer associations between decline in network measures and decline in memory functioning (RAVLT immediate: network size, clustering, gamma and lambda), while decline in most network measures (except for the path length) was associated with decline in attention/executive functioning and all network measures were related to decline on the MMSE. Additionally, decline in network measures (network size, clustering, path length, gamma and lambda) was associated with decline in language functioning in Alzheimer's disease dementia individuals.

When repeating analyses additionally accounting for the effect of whole-brain GM or hippocampal volume changes, effects for path length and lambda on decline in memory tests remained in preclinical Alzheimer's disease, and for prodromal and Alzheimer's disease dementia effects were attenuated but remained significant (Supplementary Figs 9 and 10 and Tables 15 and 16), indicating that these measures explain variance in cognitive decline in addition to GM atrophy and hippocampal atrophy.

Discussion

Our main finding is that GM network measures, particularly gamma and lambda, declined over time across the Alzheimer's disease clinical continuum, with disruptions accelerating for more advanced disease stages. Importantly, changes in these network measures were associated with concurrent decline in specific cognitive domains, which reflected the respective cognitive stage. These findings suggest that GM network measures are useful to track disease progression across the Alzheimer's disease cognitive continuum.

Previous studies using cross-sectional approaches reported disruptions in GM network measures across the clinical spectrum of Alzheimer's disease: starting in the earliest stages of Alzheimer's disease, when cognition was still intact and amyloid started aggregating (Tijms *et al.*, 2016; ten Kate *et al.*, 2018; Voevodskaya *et al.*, 2018), showing intermediate disruptions for prodromal Alzheimer's disease as compared to CN and Alzheimer's disease dementia individuals (Yao *et al.*, 2010; Pereira *et al.*, 2016) and being associated with the rate of future cognitive decline in preclinical (Verfaillie *et al.*, 2018) and prodromal Alzheimer's disease (Dicks *et al.*, 2018), and with cognitive impairment in the dementia stage (Tijms

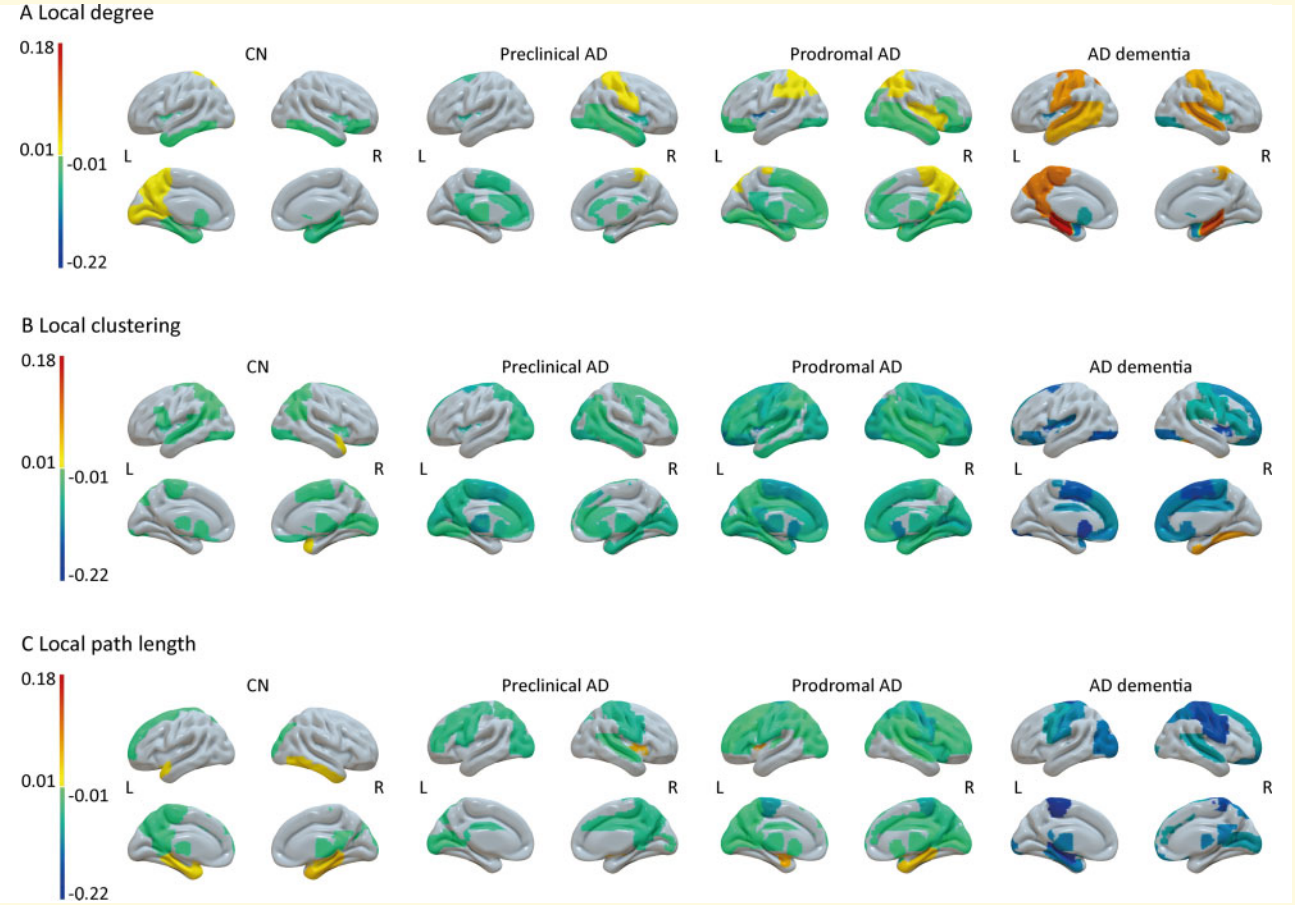

Figure 4 Surface plots of longitudinal effects in regional network measures by baseline disease stage. Longitudinal changes in local degree (**A**), local clustering (**B**) and local path length (**C**) are based on estimated marginal trends as modelled with Bayesian linear mixed models. Effects were considered significant if the 95% credible interval did not cross zero. Group differences were considered significant if the 95% credible interval of the pairwise group comparison did not cross zero and effects for the respective groups were significant. For differences between baseline disease stages, see Supplementary Fig. 7. Subcortical structures are plotted in ventricular areas as approximation. L, left hemisphere; R, right hemisphere.

et al., 2013a, 2014). Here, using a longitudinal approach, we extend on those results by showing in a longitudinal design that *within* individuals the rate of decline in GM network measures accelerates as the disease progresses and that those changes are associated with decline in cognition throughout the Alzheimer's disease cognitive continuum.

Network measures, most notably gamma and lambda, declined in all groups with decline accelerating in individuals in more advanced stages of the disease. For preclinical Alzheimer's disease, baseline clustering and especially gamma and lambda values were already lower than in CN individuals, suggesting that GM network disruptions manifest in the earliest stage of Alzheimer's disease. Additionally, decline in clustering and gamma values over time was slightly faster in preclinical Alzheimer's disease than for CN individuals. Lower clustering values have previously been related to lower CSF amyloid levels (Tijms *et al.*, 2016) and higher amyloid PET SUVR (ten Kate *et al.*, 2018) mostly within the normal range in cognitively normal individuals. Presumably, early synaptic dysfunction due to amyloid aggregation renders GM morphology more dissimilar at a regional level, resulting in lower clustering and gamma values already in the preclinical stage. We further observed that decline in network measures was accelerated with higher tau levels in the preclinical and prodromal Alzheimer's disease stage. This suggests that high levels of tau may exacerbate the disruption of GM networks in the predementia stages of the disease. Future studies should further investigate the association between network measures and tau with e.g. tau PET.

In line with the results for global network measures, local associations showed that already in the preclinical stage clustering values were lower compared to CN mostly in the temporal lobes. Over time, clustering values declined in widespread regions, which extended to frontal and parietal areas. Potentially, local early

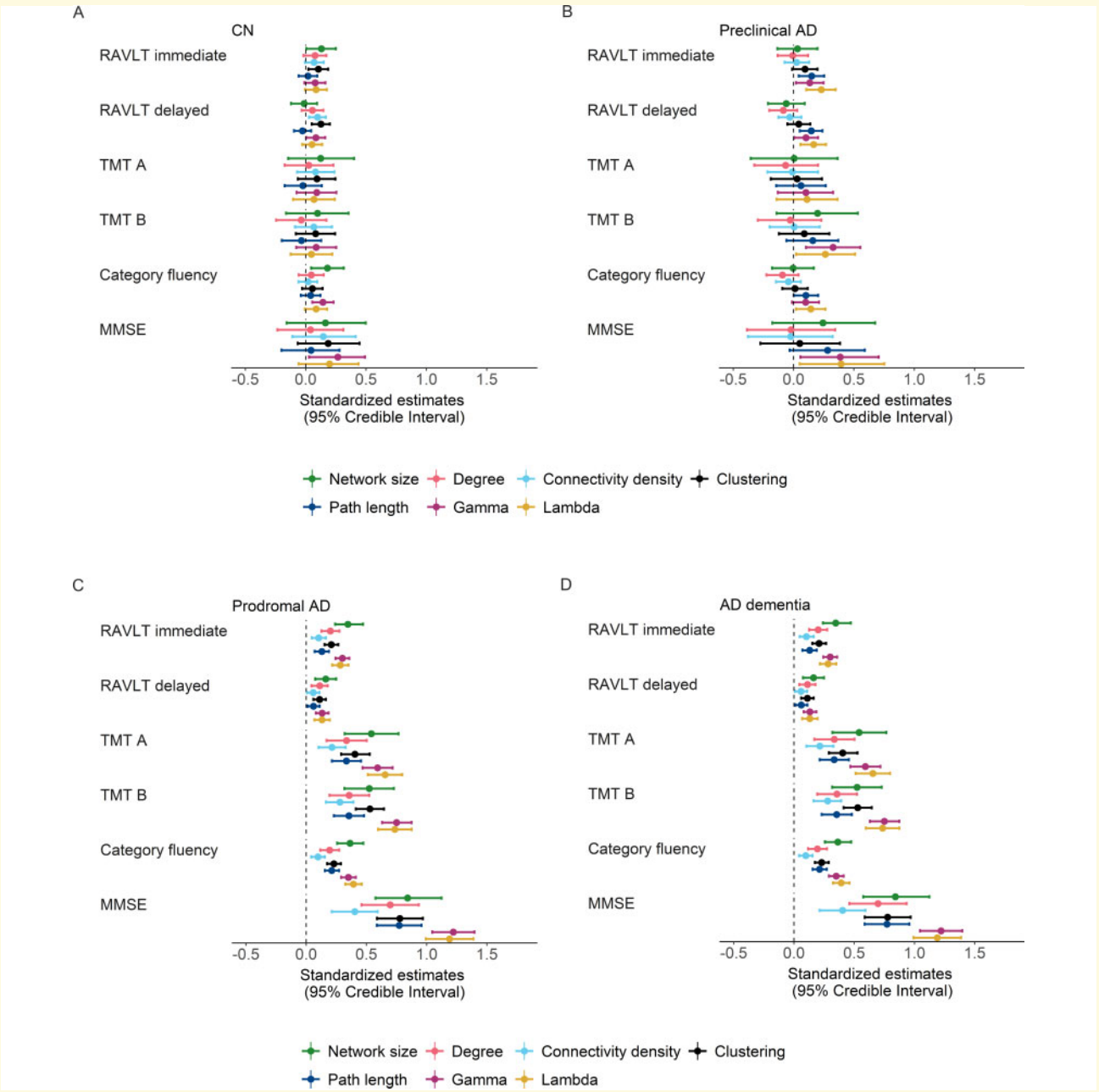

Figure 5 Within-individual associations of declines in global network measures and cognition by baseline disease stage. Effects of network measures on cognitive decline in CN (**A**), preclinical AD (**B**), prodromal AD (**C**) and AD dementia individuals (**D**) are based on estimated marginal trends as modelled with Bayesian linear mixed models. The error bars represent 95% credible intervals. Effects were considered significant if the 95% credible interval did not cross zero. Group differences were considered significant if the 95% credible interval of the pairwise group comparison did not cross zero and effects for the respective groups were significant. Estimates can additionally be found in Supplementary Table 14. AD, Alzheimer's disease. Gamma is normalized clustering; lambda is normalized path length.

neurodegenerative changes may cause large-scale disruptions network-wide, presumably due to lack of stimulation and/or neurotrophic factors from connecting regions (Salehi *et al.*, 2006; Seeley *et al.*, 2009). Additionally, while local path length values showed a similar widespread anatomical pattern of decline, this decline was observed for spatially separate regions from those of clustering, which suggests that clustering and path length may capture distinct aspects of ongoing neurodegenerative processes. In preclinical Alzheimer's disease individuals, decline in network measures, most prominently gamma and lambda, was furthermore associated with concurrent decline on the MMSE and in memory functioning, which is in line with the observation that

memory functioning is the first cognitive domain to be affected in (typical) Alzheimer's disease (Scheltens *et al.*, 2016). A practical implication of these findings is that network measures, and especially gamma, might be used to monitor disease worsening from the earliest stages of Alzheimer's disease, which is important for the development of new therapies in clinical trials.

For prodromal Alzheimer's disease and Alzheimer's disease dementia, baseline network measures were more decreased and decline in network measures markedly accelerated, suggesting that as neuronal damage becomes more widespread in later stages of disease, networks become increasingly random, as indicated by a rapid decline in small-world values, in line with previous cross-sectional studies in Alzheimer's disease (He *et al.*, 2008; Yao *et al.*, 2010, Tijms *et al.*, 2013a, *b*; Pereira *et al.*, 2016). In these individuals, local network measures at baseline were mostly decreased compared to preclinical Alzheimer's disease, and for prodromal Alzheimer's disease showed widespread and slightly steeper annual decline, particular for local clustering values. Unexpectedly, we observed for individuals with Alzheimer's disease dementia an increase in local degree, concerning mostly parietal and medial temporal regions that overlapped with a decline in local path length values. Possibly, this increase indicates that neurodegeneration starts to affect almost the entire cortex in the dementia stage of Alzheimer's disease, which leads to increased similarity between brain areas due to atrophy and causes an increase in random connections in GM networks as suggested by the concurrent decline in normalized path length.

In individuals with prodromal Alzheimer's disease, decline in all network measures was associated with concurrent decline in all cognitive tests and showed the strongest effects across all groups. This finding may indicate how continuing neuronal loss, as reflected by the disruption in network measures, gives rise to the cognitive dysfunction as seen in Alzheimer's disease, particularly in the prodromal stage. In Alzheimer's disease dementia individuals, these associations were again reduced for most cognitive tests, possibly reflecting floor effects in cognitive and neurodegenerative decline in the dementia stage of the disease. However, associations with decline on non-memory domains and global cognition became stronger in this group, suggesting that network measures might still have use to monitor disease severity in this stage and might thus aid in the development of tertiary prevention trials.

Network measures also declined in CN individuals, who had normal amyloid levels based on PET, and these changes were associated with concurrent decline in memory, language functioning and on the MMSE. This suggests that with normal aging, networks also become more randomly organized, albeit at much slower rates than in Alzheimer's disease, and that these changes are associated with decline in cognition during normal ageing. Alternatively, subthreshold effects of abnormal amyloid in CSF may explain at least some of the decline in network measures we observed in CN individuals. Additional *post hoc* analyses showed that indeed individuals with lower, but still mostly normal CSF amyloid levels already showed decline in degree (Supplementary Tables 17 and 18). However, longer follow-up is necessary to determine how many individuals developed abnormal amyloid, and whether their network organization further declines to resemble those in the preclinical stage. Previous cross-sectional studies on normal aging have reported both reorganization of brain networks towards a more regular (i.e. high clustering, high path length) and towards a more random (i.e. low clustering, low path length) topology (Chen *et al.*, 2011; Wu *et al.*, 2012, 2013; Zhu *et al.*, 2012; Carey *et al.*, 2019). Cross-sectional studies only capture a moment in time of a sample of individuals, and cohort effects might explain the conflicting results previously reported. Here, using a longitudinal approach, our results of declining gamma and lambda values in CN support the finding of brain networks reorganizing towards a more random topology in older age. Additional *post hoc* analyses showed that while older individuals had lower baseline network measures, the rate of decline in network measures was not associated with age (Supplementary Table 19), suggesting that network measures decline linearly with advancing age. Future studies should further aim to clarify how network measures change within 'healthy' individuals across a wider lifespan. Our finding of associations between network measures and concurrent changes in cognition in cognitively unimpaired normal older individuals also supports the idea that network measures may provide a biological substrate for cognitive dysfunction during normal ageing.

A potential limitation is that we modelled changes in network measures over disease advancement using follow-up time as predictor, which may not adequately capture where individuals are in their own disease trajectory (Bateman *et al.*, 2012; Insel *et al.*, 2017; Vogel *et al.*, 2018), and as such slope estimates based on time may be overestimated (Dicks *et al.*, 2019). Still, modelling concurrent changes in GM network measures and cognitive dysfunction, we showed that network measures are closely related to disease advancement within individuals, and thus network measures may inform on an individual's precise disease stage. Additionally, we used individual neuropsychological tests to investigate the association of declines in network measures and cognition. Composite scores may outperform their single components in assessing cognitive decline over time and may show stronger associations with neuroimaging markers (Crane *et al.*, 2012; Gibbons *et al.*, 2012). However, using individual tests as outcome measures eases interpretation of results and comparison across different cognitive stages. Another potential limitation of our study is that we prioritized amyloid PET to determine amyloid positivity, and in this

way included some individuals in the Alzheimer's disease continuum although they had normal amyloid in CSF. This may have attenuated some of the results, but, since the percentage of individuals with discordant amyloid was low (13% for preclinical, 4% for prodromal Alzheimer's disease), such effects are likely to be minimal. Strengths of our study include the large number of participants from ADNI who had long follow-up duration of up to 10 years with repeated MRI available. Using our approach to construct single-subject GM networks furthermore enabled us to investigate declines in network measures and cognition and their associations on an individual participant data level, in contrast to group-level network measures. Additionally, GM networks are reconstructed from structural MRI, which are routinely acquired in large research cohorts and clinical practice, are less affected by artefacts, and their acquisition and processing are less time-consuming than those for other sequences.

In conclusion, we showed that network measures continuously decline over time within individuals, and that the rate of decline accelerates for individuals in more advanced stages of the disease. Changes in network measures were associated with concurrent cognitive decline across the entire Alzheimer's disease continuum, suggesting that GM network measures may have use to help monitoring disease progression in Alzheimer's disease.

Supplementary material

Supplementary material is available at *Brain Communications* online.

Acknowledgements

ADNI acknowledgements: Data collection and sharing for this project was funded by the Alzheimer's Disease Neuroimaging Initiative (ADNI) (National Institutes of Health Grant U01 AG024904) and DOD ADNI (Department of Defense award number W81XWH-12-2-0012). ADNI is funded by the National Institute on Aging, the National Institute of Biomedical Imaging and Bioengineering, and through generous contributions from the following: AbbVie, Alzheimer's Association; Alzheimer's Drug Discovery Foundation; Araclon Biotech; BioClinica, Inc.; Biogen; Bristol-Myers Squibb Company; CereSpir, Inc.; Cogstate; Eisai Inc.; Elan Pharmaceuticals, Inc.; Eli Lilly and Company; EuroImmun; F. Hoffmann-La Roche Ltd and its affiliated company Genentech, Inc.; Fujirebio; GE Healthcare; IXICO Ltd.; Janssen Alzheimer Immunotherapy Research & Development, LLC.; Johnson & Johnson Pharmaceutical Research & Development LLC.; Lumosity; Lundbeck; Merck & Co., Inc.; Meso Scale Diagnostics, LLC.; NeuroRx Research; Neurotrack Technologies; Novartis Pharmaceuticals Corporation; Pfizer Inc.; Piramal Imaging; Servier; Takeda Pharmaceutical Company; and Transition Therapeutics. The Canadian Institutes of Health Research is providing funds to support ADNI clinical sites in Canada. Private sector contributions are facilitated by the Foundation for the National Institutes of Health (www.fnih.org). The grantee organization is the Northern California Institute for Research and Education, and the study is coordinated by the Alzheimer's Therapeutic Research Institute at the University of Southern California. ADNI data are disseminated by the Laboratory for Neuro Imaging at the University of Southern California.

Funding

This work was supported by the ZonMw Memorabel Grant Program (BMT; grant number 73305056). Research of the Alzheimer Center Amsterdam is part of the neurodegeneration research programme of Amsterdam Neuroscience. WvdF holds the Pasman chair. The Alzheimer Center Amsterdam is supported by Stichting Alzheimer Nederland and Stichting VUmc Fonds.

Competing interests

E.D. and L.V. report no competing interests. W.M.v.d.F.'s research programmes have been funded by ZonMW, NWO, EU-FP7, EU-JPND, Alzheimer Nederland, CardioVascular Onderzoek Nederland, Health~Holland, Topsector Life Sciences & Health, stichting Dioraphte, Gieskes-Strijbis fonds, stichting Equilibrio, Pasman stichting, Biogen MA Inc, Boehringer Ingelheim, Life-MI, AVID, Roche BV, Janssen Stellar, Combinostics. W.M.v.d.F. holds the Pasman chair. W.M.v.d.F. has performed contract research for Biogen MA Inc. and Boehringer Ingelheim. W.M.v.d.F. has been an invited speaker at Boehringer Ingelheim and Biogen MA Inc. All funding is paid to her institution. F.B. is a consultant for Biogen-Idec, Janssen Alzheimer Immunotherapy, Bayer-Schering, Merck-Serono, Roche, Novartis, Genzume and Sanofi-Aventis; has received sponsoring from European Commission–Horizon 2020, National Institute for Health Research–University College London Hospitals Biomedical Research Centre, Scottish Multiple Sclerosis Register, TEVA, Novartis and Toshiba; is supported by the University College London Hospitals NHS Foundation Trust Biomedical Research Center; and serves on the editorial boards of Radiology, Brain, Neuroradiology, Multiple Sclerosis Journal and Neurology. P.S. has acquired grant support (for the institution) from BiogenGE Healthcare, Danone Research, Piramal and Merck. In the past 2 years, he has received consultancy/speaker fees (paid to the institution) from Lilly, GE Healthcare, Novartis, Sanofi, Nutricia, Probiodrug, Biogen, Roche, Avraham and EIP Pharma, Merck AG. B.M.T. received grant support from ZonMw Memorabel (grant number 73305056).

References

Alexander-Bloch A, Giedd JN, Bullmore E. Imaging structural co-variance between human brain regions. Nat Rev Neurosci 2013a; 14: 322–36.

Alexander-Bloch A, Raznahan A, Bullmore E, Giedd J. The convergence of maturational change and structural covariance in human cortical networks. J Neurosci 2013b; 33: 2889–99.

Bateman RJ, Xiong C, Benzinger TL, Fagan AM, Goate A, Fox NC, et al. Clinical and biomarker changes in dominantly inherited Alzheimer's disease. N Engl J Med 2012; 367: 795–804.

Buckner RL, Snyder AZ, Shannon BJ, LaRossa G, Sachs R, Fotenos AF, et al. Molecular, structural, and functional characterization of Alzheimer's disease: evidence for a relationship between default activity, amyloid, and memory. J Neurosci 2005; 25: 7709–17.

Carey D, Nolan H, Kenny RA, Meaney J. Cortical covariance networks in ageing: cross-sectional data from the Irish Longitudinal Study on Ageing (TILDA). Neuropsychologia 2019; 122: 51–61.

Chen ZJ, He Y, Rosa-Neto P, Gong G, Evans AC. Age-related alterations in the modular organization of structural cortical network by using cortical thickness from MRI. Neuroimage 2011; 56: 235–45.

Crane PK, Carle A, Gibbons LE, Insel P, Mackin RS, Gross A, et al.; for the Alzheimer's Disease Neuroimaging Initiative. Development and assessment of a composite score for memory in the Alzheimer's Disease Neuroimaging Initiative (ADNI). Brain Imaging Behav 2012; 6: 502–16.

Dickerson BC, Bakkour A, Salat DH, Feczko E, Pacheco J, Greve DN, et al. The cortical signature of Alzheimer's disease: regionally specific cortical thinning relates to symptom severity in very mild to mild AD dementia and is detectable in asymptomatic amyloid-positive individuals. Cereb Cortex 2009; 19: 497–510.

Dicks E, Tijms BM, Ten Kate M, Gouw AA, Benedictus MR, Teunissen CE, et al. Gray matter network measures are associated with cognitive decline in mild cognitive impairment. Neurobiol Aging 2018; 61: 198–206.

Dicks E, Vermunt L, van der Flier WM, Visser PJ, Barkhof F, Scheltens P, et al. Modeling grey matter atrophy as a function of time, aging or cognitive decline show different anatomical patterns in Alzheimer's disease. Neuroimage Clin 2019; 22: 101786.

Dubois B, Epelbaum S, Nyasse F, Bakardjian H, Gagliardi G, Uspenskaya O, et al. Cognitive and neuroimaging features and brain beta-amyloidosis in individuals at risk of Alzheimer's disease (INSIGHT-preAD): a longitudinal observational study. Lancet Neurol 2018; 17: 335–46.

Farrell ME, Kennedy KM, Rodrigue KM, Wig G, Bischof GN, Rieck JR, et al. Association of longitudinal cognitive decline with amyloid burden in middle-aged and older adults: evidence for a dose-response relationship. JAMA Neurol 2017; 74: 830–8.

Folstein MF, Folstein SE, McHugh PR. 'Mini-mental state'. A practical method for grading the cognitive state of patients for the clinician. J Psychiatr Res 1975; 12: 189–98.

Fox NC, Scahill RI, Crum WR, Rossor MN. Correlation between rates of brain atrophy and cognitive decline in AD. Neurology 1999; 52: 1687.

Gelman A, Rubin DB. Inference from iterative simulation using multiple sequences. Statist Sci 1992; 7: 457–72.

Gelman A, Shirley K. Inference from simulations and monitoring convergence. In: A Gelman, Meng X-L, Jones G, Brooks S, editors. Handbook of Markov Chain Monte Carlo. Vol. 6. New York: CRC Press; 2011. p. 163–74.

Gibbons LE, Carle AC, Mackin RS, Harvey D, Mukherjee S, Insel P, et al.; for the Alzheimer's Disease Neuroimaging Initiative. A composite score for executive functioning, validated in Alzheimer's Disease Neuroimaging Initiative (ADNI) participants with baseline mild cognitive impairment. Brain Imaging Behav 2012; 6: 517–27.

Gong G, He Y, Chen ZJ, Evans AC. Convergence and divergence of thickness correlations with diffusion connections across the human cerebral cortex. Neuroimage 2012; 59: 1239–48.

Goodrich B, Gabry J, Ali I, Brilleman S, rstanarm: Bayesian applied regression modeling via Stan. [Internet]. 2020. https://mc-stan.org/rstanarm (2 November 2020, date last accessed).

He Y, Chen Z, Evans A. Structural insights into aberrant topological patterns of large-scale cortical networks in Alzheimer's disease. J Neurosci 2008; 28: 4756–66.

Insel PS, Ossenkoppele R, Gessert D, Jagust W, Landau S, Hansson O, et al. Time to amyloid positivity and preclinical changes in brain metabolism, atrophy, and cognition: evidence for emerging amyloid pathology in Alzheimer's disease. Front Neurosci 2017; 11: 1–9.

Jack CR, Bernstein MA, Fox NC, Thompson P, Alexander G, Harvey D, et al. The Alzheimer's Disease Neuroimaging Initiative (ADNI): MRI methods. J Magn Reson Imaging 2008; 27: 685–91.

Jack CR, Petersen RC, Xu Y, O'Brien PC, Smith GE, Ivnik RJ, et al. Rates of hippocampal atrophy correlate with change in clinical status in aging and AD. Neurology 2000; 55: 484–89.

Jagust WJ, Bandy D, Chen K, Foster NL, Landau SM, Mathis CA, et al. The Alzheimer's Disease Neuroimaging Initiative positron emission tomography core. Alzheimers Dement 2010; 6: 221–9.

Jagust WJ, Landau SM, Koeppe RA, Reiman EM, Chen K, Mathis CA, et al. The Alzheimer's Disease Neuroimaging Initiative 2 PET Core: 2015. Alzheimers Dement 2015; 11: 757–71.

Jansen WJ, Ossenkoppele R, Knol DL, Tijms BM, Scheltens P, Verhey FR, et al. Prevalence of cerebral amyloid pathology in persons without dementia: a meta-analysis. JAMA 2015; 313: 1924–38.

Koffie RM, Meyer-Luehmann M, Hashimoto T, Adams KW, Mielke ML, Garcia-Alloza M, et al. Oligomeric amyloid beta associates with postsynaptic densities and correlates with excitatory synapse loss near senile plaques. Proc Natl Acad Sci U S A 2009; 106: 4012–7.

Lenth R. emmeans: Estimated Marginal Means, aka Least-Squares Means. 2018. https://cran.r-project.org/web/packages/emmeans/emmeans.pdf (2 November 2020, date last accessed).

Maslov SS, Sneppen K. Specificity and stability in topology of protein networks. Science 2002; 296: 910–3.

McKhann G, Drachman D, Folstein M, Katzman R, Price D, Stadlan EM. Clinical diagnosis of Alzheimer's disease: report of the NINCDS-ADRDA Work Group under the auspices of Department of Health and Human Services Task Force on Alzheimer's Disease. Neurology 1984; 34: 939–44.

Mechelli A, Friston KJ, Frackowiak RS, Price CJ. Structural covariance in the human cortex. J Neurosci 2005; 25: 8303–10.

Palmqvist S, Scholl M, Strandberg O, Mattsson N, Stomrud E, Zetterberg H, et al. Earliest accumulation of beta-amyloid occurs within the default-mode network and concurrently affects brain connectivity. Nat Commun 2017; 8: 1214.

Pereira JB, Mijalkov M, Kakaei E, Mecocci P, Vellas B, Tsolaki M, et al. Disrupted network topology in patients with stable and progressive mild cognitive impairment and Alzheimer's disease. Cereb Cortex 2016; 26: 3476–93.

Petersen RC, Aisen PS, Beckett LA, Donohue MC, Gamst AC, Harvey DJ, et al. Alzheimer's Disease Neuroimaging Initiative (ADNI): clinical characterization. Neurology 2010; 74: 201–9.

Reitan RM. Validity of the Trail Making Test as an indicator of organic brain damage. Percept Mot Skills 1958; 8: 271–276.

Reuter M, Schmansky NJ, Rosas HD, Fischl B. Within-subject template estimation for unbiased longitudinal image analysis. Neuroimage 2012; 61: 1402–18.

Rey A. L'examen clinique en psychologie. Paris, France: Presses Universitaires de France; 1964.

Rubinov M, Sporns O. Complex network measures of brain connectivity: uses and interpretations. Neuroimage 2010; 52: 1059–69.

Salehi A, Delcroix JD, Belichenko PV, Zhan K, Wu C, Valletta JS, et al. Increased App expression in a mouse model of Down's syndrome disrupts NGF transport and causes cholinergic neuron degeneration. Neuron 2006; 51: 29–42.

Scheltens P, Blennow K, Breteler MM, de Strooper B, Frisoni GB, Salloway S, et al. Alzheimer's disease. Lancet 2016; 388: 505–17.

Seeley WW, Crawford RK, Zhou J, Miller BL, Greicius MD. Neurodegenerative diseases target large-scale human brain networks. Neuron 2009; 62: 42–52.

Selkoe DJ. Alzheimer's disease is a synaptic failure. Science 2002; 298: 789–91.

Shankar GM, Li S, Mehta TH, Garcia-Munoz A, Shepardson NE, Smith I, et al. Amyloid-beta protein dimers isolated directly from Alzheimer's brains impair synaptic plasticity and memory. Nat Med 2008; 14: 837–42.

Shaw LM, Vanderstichele H, Knapik-Czajka M, Clark CM, Aisen PS, Petersen RC, et al.; Alzheimer's Disease Neuroimaging Initiative. Cerebrospinal fluid biomarker signature in Alzheimer's disease neuroimaging initiative subjects. Ann Neurol 2009; 65: 403–13.

Sperling RA, LaViolette PS, O'Keefe K, O'Brien J, Rentz DM, Pihlajamaki M, et al. Amyloid deposition is associated with impaired default network function in older persons without dementia. Neuron 2009; 63: 178–88.

ten Kate M, Visser PJ, Bakardjian H, Barkhof F, Sikkes SAM, van der Flier WM, et al. Gray matter network disruptions and regional amyloid beta in cognitively normal adults. Front Aging Neurosci 2018; 11: 1–11.

Tijms BM, Möller C, Vrenken H, Wink AM, de Haan W, van der Flier WM, et al. Single-subject grey matter graphs in Alzheimer's disease. PLoS One 2013a; 8: e58921.

Tijms BM, Series P, Willshaw DJ, Lawrie SM. Similarity-based extraction of individual networks from gray matter MRI scans. Cereb Cortex 2012; 22: 1530–41.

Tijms BM, Ten Kate M, Gouw AA, Borta A, Verfaillie S, Teunissen CE, et al. Gray matter networks and clinical progression in subjects with predementia Alzheimer's disease. Neurobiol Aging 2018; 61: 75–81.

Tijms BM, ten Kate M, Wink AM, Visser PJ, Ecay M, Clerigue M, et al. Gray matter network disruptions and amyloid beta in cognitively normal adults. Neurobiol Aging 2016; 37: 154–60.

Tijms BM, Wink AM, de Haan W, van der Flier WM, Stam CJ, Scheltens P, et al. Alzheimer's disease: connecting findings from graph theoretical studies of brain networks. Neurobiol Aging 2013b; 34: 2023–36.

Tijms BM, Yeung HM, Sikkes SA, Moller C, Smits LL, Stam CJ, et al. Single-subject gray matter graph properties and their relationship with cognitive impairment in early- and late-onset Alzheimer's disease. Brain Connect 2014; 4: 337–46.

Tzourio-Mazoyer N, Landeau B, Papathanassiou D, Crivello F, Etard O, Delcroix N, et al. Automated anatomical labeling of activations in SPM using a macroscopic anatomical parcellation of the MNI MRI single-subject brain. Neuroimage 2002; 15: 273–89.

Verfaillie SCJ, Slot RER, Dicks E, Prins ND, Overbeek JM, Teunissen CE, et al. A more randomly organized grey matter network is associated with deteriorating language and global cognition in individuals with subjective cognitive decline. Hum Brain Mapp 2018; 39: 3143–51.

Villain N, Chetelat G, Grassiot B, Bourgeat P, Jones G, Ellis KA, et al. Regional dynamics of amyloid-beta deposition in healthy elderly, mild cognitive impairment and Alzheimer's disease: a voxelwise PiB-PET longitudinal study. Brain 2012; 135: 2126–39.

Villeneuve S, Rabinovici GD, Cohn-Sheehy BI, Madison C, Ayakta N, Ghosh PM, et al. Existing Pittsburgh Compound-B positron emission tomography thresholds are too high: statistical and pathological evaluation. Brain 2015; 138: 2020–33.

Voevodskaya O, Pereira JB, Volpe G, Lindberg O, Stomrud E, van Westen D, et al. Altered structural network organization in cognitively normal individuals with amyloid pathology. Neurobiol Aging 2018; 64: 15–24.

Vogel JW, Vachon-Presseau E, Pichet Binette A, Tam A, Orban P, La Joie R, et al. Brain properties predict proximity to symptom onset in sporadic Alzheimer's disease. Brain 2018; 141: 1871–83.

Walsh DM, Klyubin I, Fadeeva JV, Cullen WK, Anwyl R, Wolfe MS, et al. Naturally secreted oligomers of amyloid beta protein potently inhibit hippocampal long-term potentiation in vivo. Nature 2002; 416: 535–9.

Whitwell JL, Przybelski SA, Weigand SD, Knopman DS, Boeve BF, Petersen RC, et al. 3D maps from multiple MRI illustrate changing atrophy patterns as subjects progress from mild cognitive impairment to Alzheimer's disease. Brain 2007; 130: 1777–86.

Wu K, Taki Y, Sato K, Kinomura S, Goto R, Okada K, et al. Age-related changes in topological organization of structural brain networks in healthy individuals. Hum Brain Mapp 2012; 33: 552–68.

Wu K, Taki Y, Sato K, Qi H, Kawashima R, Fukuda H. A longitudinal study of structural brain network changes with normal aging. Front Hum Neurosci 2013; 7: 1–12.

Yao Z, Zhang Y, Lin L, Zhou Y, Xu C, Jiang T, the Alzheimer's Disease Neuroimaging Initiative. Abnormal cortical networks in mild cognitive impairment and Alzheimer's disease. PLoS Comput Biol 2010; 6: e1001006.

Zhu W, Wen W, He Y, Xia A, Anstey KJ, Sachdev P. Changing topological patterns in normal aging using large-scale structural networks. Neurobiol Aging 2012; 33: 899–913.